Molecular signatures of circulating melanoma cells for monitoring early response to immune checkpoint therapy

Xin Hong[a,1], Ryan J. Sullivan[a,b,1], Mark Kalinich[a], Tanya Todorova Kwan[a], Anita Giobbie-Hurder[c], Shiwei Pan[a], Joseph A. LiCausi[a], John D. Milner[a], Linda T. Nieman[a], Ben S. Wittner[a], Uyen Ho[a], Tianqi Chen[c], Ravi Kapur[d], Donald P. Lawrence[a,b], Keith T. Flaherty[a,b], Lecia V. Sequist[a,b], Sridhar Ramaswamy[a,b], David T. Miyamoto[a,e], Michael Lawrence[a], Mehmet Toner[d,f], Kurt J. Isselbacher[a,2], Shyamala Maheswaran[a,f,2], and Daniel A. Haber[a,g,2]

[a]Massachusetts General Hospital Cancer Center, Harvard Medical School, Boston, MA 02114; [b]Division of Hematology–Oncology, Massachusetts General Hospital, Harvard Medical School, Boston, MA 02114; [c]Division of Biostatistics, Dana Farber Cancer Institute, Harvard Medical School, Boston, MA 02215; [d]Center for Bioengineering in Medicine, Massachusetts General Hospital and Shriners Hospital for Children, Harvard Medical School, Boston, MA 02114; [e]Department of Radiation Oncology, Massachusetts General Hospital, Harvard Medical School, Boston, MA 02114; [f]Department of Surgery, Massachusetts General Hospital, Harvard Medical School, Boston, MA 02114; and [g]Howard Hughes Medical Institute, Chevy Chase, MD 20815

Contributed by Kurt J. Isselbacher, January 18, 2018 (sent for review November 8, 2017; reviewed by Jonathan Licht and Ben Stanger)

A subset of patients with metastatic melanoma have sustained remissions following treatment with immune checkpoint inhibitors. However, analyses of pretreatment tumor biopsies for markers predictive of response, including PD-1 ligand (PD-L1) expression and mutational burden, are insufficiently precise to guide treatment selection, and clinical radiographic evidence of response on therapy may be delayed, leading to some patients receiving potentially ineffective but toxic therapy. Here, we developed a molecular signature of melanoma circulating tumor cells (CTCs) to quantify early tumor response using blood-based monitoring. A quantitative 19-gene digital RNA signature (CTC score) applied to microfluidically enriched CTCs robustly distinguishes melanoma cells, within a background of blood cells in reconstituted and in patient-derived ($n = 42$) blood specimens. In a prospective cohort of 49 patients treated with immune checkpoint inhibitors, a decrease in CTC score within 7 weeks of therapy correlates with marked improvement in progression-free survival [hazard ratio (HR), 0.17; $P = 0.008$] and overall survival (HR, 0.12; $P = 0.04$). Thus, digital quantitation of melanoma CTC-derived transcripts enables serial noninvasive monitoring of tumor burden, supporting the rational application of immune checkpoint inhibition therapies.

circulating tumor cells | liquid biopsy | predictive biomarker | melanoma | immune checkpoint inhibition

The treatment of metastatic melanoma has been revolutionized by the development of BRAF and MEK inhibitors for patients with *BRAF*-mutant tumors (1–3), and by the immune checkpoint inhibitors against CTLA4 (ipilimumab) and PD1 (pembrolizumab, nivolumab), which are used independent of *BRAF* mutational status (4–8). Responses to targeting mutant *BRAF* are frequently profound, albeit transient, whereas immune checkpoint inhibitors lead to durable responses but only in a subset of patients (9, 10). In the absence of predictive markers of response to immunotherapy, treatment choices are empiric and further complicated by the often delayed radiographic evidence of clinical response (11). Independent of tumor response, immune checkpoint activation may be associated with severe autoimmune side effects involving the gastrointestinal tract, lung, heart, and endocrine organs.

Analysis of tumor biopsies has suggested a number of features that are correlated with response to immune checkpoint inhibitors, although none appears sufficiently reliable to direct treatment choices. Elevated tumor or stromal expression of the PD-1 ligand (PD-L1) is partially predictive of response to PD-1 inhibitors, and tumor expression of mesenchymal markers may be associated with poor clinical outcome (12–15). Overall mutational burden is correlated with the number of predicted neoepitopes and with response to immunotherapy, especially in colorectal and lung cancers (16, 17), while UV damage-associated mutational signatures have been correlated with response in melanoma (18, 19). Following initiation of checkpoint inhibitor therapy, repeated tumor biopsies showing increased T-cell receptor (TCR) clonality or expression of immune cytolytic markers are associated with response (20). However promising, serial tumor biopsies are invasive and only sample a single metastatic site, which may not be representative of the entire tumor burden in a highly heterogeneous cancer such as melanoma. Thus, there is an unmet need for noninvasive blood-based markers that may integrate signals from all metastatic foci and which can be repeated serially during the course of treatment.

Significance

Identifying predictive biomarkers of therapeutic response for melanoma patients treated with immune checkpoint inhibitors is a major challenge. By combining microfluidic enrichment for melanoma circulating tumor cells (CTCs) together with RNA-based droplet digital PCR quantitation, we have established a highly sensitive and robust platform for noninvasive, blood-based monitoring of tumor burden. Serial monitoring of melanoma patients treated with immune checkpoint inhibitors shows rapid changes in CTC score, which precede standard clinical assessment and are highly predictive of long-term clinical outcome. Early on-treatment digital monitoring of CTC dynamics may thus help identify patients likely to benefit from immune checkpoint inhibition therapy.

Author contributions: X.H., R.J.S., S.M., and D.A.H. designed research; X.H., R.J.S., M.K., T.T.K., S.P., J.A.L., J.D.M., L.T.N., B.S.W., U.H., and D.T.M. performed research; R.K. contributed new reagents/analytic tools; X.H., R.J.S., M.K., T.T.K., A.G.-H., S.P., J.A.L., J.D.M., L.T.N., B.S.W., U.H., T.C., D.P.L., K.T.F., L.V.S., S.R., D.T.M., M.L., M.T., K.J.I., S.M., and D.A.H. analyzed data; and X.H., R.J.S., A.G.-H., T.C., R.K., D.P.L., K.T.F., M.L., M.T., K.J.I., S.M., and D.A.H. wrote the paper.

Reviewers: J.L., University of Florida; and B.S., University of Pennsylvania.

Conflict of interest statement: Massachusetts General Hospital and the authors have applied for patent protection for the CTC-iChip technology and the molecular signatures of melanoma cells.

Data deposition: The R script used to generate these analyses is available at Github (https://github.com/markkalinich/dPCR).

[1]X.H. and R.J.S. contributed equally to this work.

[2]To whom correspondence may be addressed. Email: kisselbacher@mgh.harvard.edu, maheswaran@helix.mgh.harvard.edu, or dhaber@mgh.harvard.edu.

This article contains supporting information online at www.pnas.org/lookup/suppl/doi:10.1073/pnas.1719264115/-/DCSupplemental.

Published online February 16, 2018.

Circulating tumor cells (CTCs) are shed into the bloodstream from either primary or metastatic cancer deposits. However, classical CTC isolation technologies rely upon their capture through expression of the epithelial surface protein EpCAM, which is absent in melanoma cells (21, 22), and even the application of melanoma epitope-specific CTC capture identifies only small numbers of CTCs in patients with advanced disease (23). The high degree of heterogeneity among melanoma cells further exacerbates the challenge of imaging rare cancer cells admixed with contaminating leukocytes. We previously have demonstrated that high-efficiency microfluidic depletion of normal hematopoietic cells from blood samples of patients with cancer provides a highly enriched population of untagged viable CTCs, containing intact RNA (10^5-fold of enrichment; CTC capture efficiency, >97%) (24–26). This CTC enrichment platform is particularly well suited to melanoma, since it takes advantage of universal leukocyte epitopes and does not require isolation based on melanoma-specific markers. Since melanocytes are of neural crest origin, they express unique transcripts, many of which are preserved in melanomas but are absent from normal blood cells. We therefore reasoned that the application of highly sensitive and specific digital PCR detection technologies might provide a strategy for molecular quantitation of melanoma CTCs (27), following microfluidic enrichment from the blood of patients undergoing treatment. In a prospective cohort of patients receiving checkpoint immunotherapy for metastatic

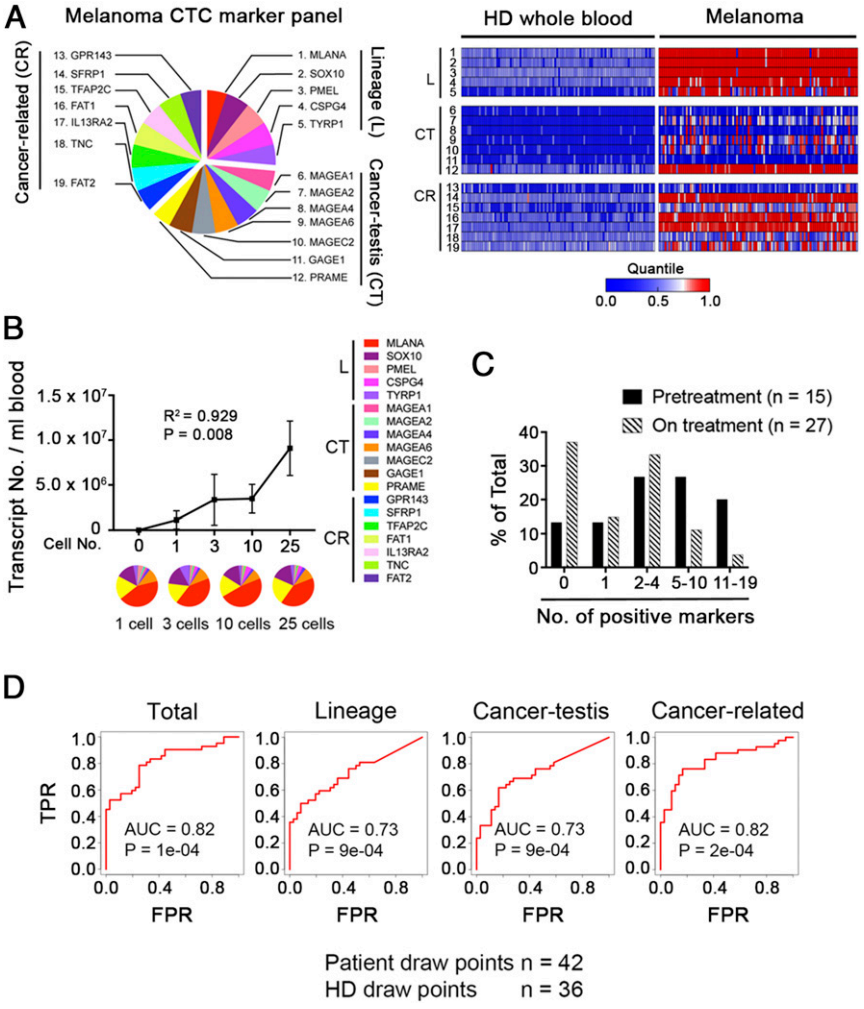

Fig. 1. Development of melanoma CTC digital scoring assay. (*A*) Marker gene selection. (*Left*) Colored pie chart of the 19 melanoma CTC markers identified from a list of candidate genes. Each marker is listed in numeric order with a color code and grouped into one out the three categories: lineage (L) (markers 1–5), cancer-testis antigen (CT) (markers 6–12), and cancer-related (CR) (markers 13–19). (*Right*) A heat map of the 19-marker gene expression by RNA sequencing of 100 healthy donor (HD) whole-blood samples (GTEx) versus 103 primary melanoma tumor samples (TCGA portal). Numbers in *y* axis refer to marker genes listed in the pie chart. Each column on the *x* axis represents a HD blood sample or melanoma. Red and blue depict high and low expression, respectively (normalized in quantile). (*B*) Detection sensitivity of the melanoma-specific digital signal. Individual melanoma (SK-ML-28) cells (0, 1, 3, 10–25 cells) were introduced into 4 mL of HD blood (containing about 20 billion blood cells), processed through the CTC-iChip, and then subjected to digital quantitation of melanoma gene transcripts listed on *Right*. Data points show the mean number of transcripts (positive droplets) for all 19 genes per mL of blood processed ± SD, derived from three independent experiments. The relatively consistent distribution of signal with increasing number of spiked cells is shown in the pie chart. (*C*) Bar graph showing number of positive CTC-derived markers in blood samples from untreated patients with metastatic melanoma ($n = 15$) and from patients actively receiving therapy ($n = 27$). The fraction of patients positive for 0, 1, 2–4, 5–10, and 11–19 markers is shown. (*D*) Test characteristics of CTC-derived transcripts in 33 melanoma patients (42 draw points), compared with 36 individual blood draws from HDs. ROC curves for prediction of melanoma were derived for all markers (total; $n = 19$), or for subsets of markers (lineage; $n = 5$, cancer-testis antigens; $n = 7$, and cancer-related transcripts; $n = 7$) using univariate logistic regression. AUC, area under the curve; FPR, false-positive rate; TPR, true-positive rate.

melanoma, we tested the clinical utility of this digital CTC assay for early prediction of treatment response.

Results

Development of a Digital RNA-Based Melanoma CTC Scoring Assay. We devised an initial screen for candidate melanoma CTC-derived transcripts distinguishable from those of contaminating blood cells, using RNA sequencing data of human melanoma samples and healthy donor (HD) white blood cell samples from The Cancer Genome Atlas (TCGA) (https://cancergenome.nih.gov) and Genotype-Tissue Expression (GTEx) (https://www.gtexportal.org) databases, followed by experimental validation of candidates using real-time quantitative PCR and digital droplet PCR methods. From 94 initial candidates, we identified 19 transcripts that are highly expressed in melanomas but below detection in normal blood cells, even at the very high level of digital PCR sensitivity (Fig. 1*A*, Fig. S1*D*, and Table S5). These markers include five melanocyte-specific lineage genes [lineage (L)], seven cancer testis antigens overexpressed in melanomas [cancer-testis (CT)], and seven other genes expressed by both melanoma and other cancer types [cancer-related (CR)]. To test the sensitivity and linearity of the CTC-derived signal, we introduced either 0, 1, 3, 10, or 25 individually micromanipulated melanoma cells (SK-MEL-28) into 4 mL of whole blood from HDs, followed by CTC-iChip processing and digital PCR quantitation. Dramatic signal amplification was observed, such that a single SK-ML-28 cell spiked into 4 mL of HD blood generated a median of 1,119,617 ± 996,836 positive transcripts (droplets) per mL of blood, compared with an unspiked background of 148 ± 121 transcripts per mL of blood (Fig. 1*B*). The total number of transcripts was well correlated with the number of cells spiked into blood ($R^2 = 0.929$, $P = 0.008$), and the relative distribution among each of the markers remained constant with increasing numbers of spiked cells. Similar results were obtained with cell-spiking experiments using a second melanoma cell line (Mel-167; Fig. S2*A*; $R^2 = 0.820$, $P = 0.034$). Given the admixture of extremely rare CTCs among abundant blood cells, initial microfluidic enrichment of tumor cells from whole blood was required for reliable detection using digital droplet-based PCR (Fig. S2*B*).

Application of the Digital CTC Assay in a Test Cohort of Melanoma Patients. To test the performance of the digital melanoma CTC assay in clinical specimens, we tested blood specimens from 33 patients with metastatic melanoma at various stages of therapy (42 draw points), compared with 36 HDs. When each marker was thresholded using HD background signal, 13 of 15 (86.7%) untreated samples and 17 of 27 (63.0%) on-treatment samples had positive signal for at least one CTC-derived RNA marker (Fig. 1*C*). To assess the sensitivity and specificity of the assay in distinguishing patients with melanoma versus HDs, we applied an univariate logistic regression model, separating melanoma patients from HDs, with areas under the curve (AUCs) ranging from 0.73 to 0.82 for lineage-specific, cancer-testis antigen, cancer-related markers, and all 19 markers together (Fig. 1*D*). Receiver operating characteristic (ROC) curves for individual markers also reached statistical significance for nine individual genes (Fig. S3). The other genes did not reach significance as individual markers, primarily due to their expression in only a subset of melanoma patient CTCs. However, their exceptional signal-to-noise ratio within the positive patient subset warranted their inclusion in the signature, given the need to capture the considerable heterogeneity of gene expression markers in melanoma. To allow longitudinal monitoring of individual patients, we established a CTC score consisting of the total number of transcripts for all 19 markers, with a threshold set at 2 SDs above the median signal for each marker across the 36 HDs (*Materials and Methods*). As shown in a patient with *B-RAF V600E*-mutant melanoma responding to targeted therapy, and in a second patient lacking such a mutation and progressing despite therapy, longitudinal measurements of CTC score are highly consistent with response or nonresponse to therapy (Fig. S4).

Serial Monitoring of CTC Score Dynamics in a Prospective Cohort of Patients Receiving Immune Checkpoint Inhibition Therapies. Having established a digital molecular assay to measure the presence of melanoma CTCs, we applied this strategy to a separate, prospective cohort of 49 patients with metastatic melanoma, who were treated with immune checkpoint inhibitors (Fig. 2*A* and

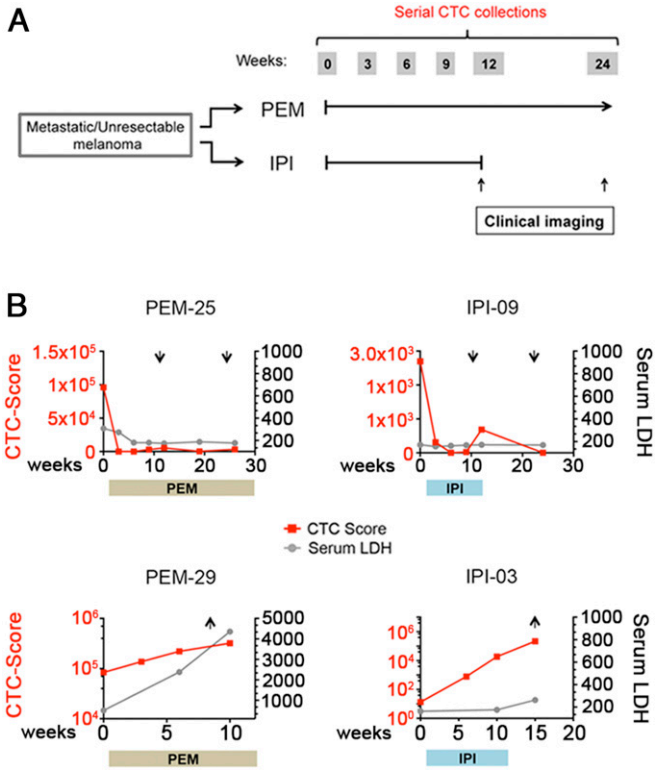

Fig. 2. Longitudinal monitoring of CTCs in patients treated with immune checkpoint inhibition therapies. (*A*) Schematic diagram showing serial CTC collection and clinical imaging of melanoma patients receiving immunotherapy. Forty-nine patients with metastatic or unresectable melanoma were treated with either pembrolizumab ($n = 33$) or ipilimumab ($n = 16$). CTCs were serially collected at 0, 3, 6, 9, 12, and 24 wk, or any close time points that were available. Routine clinical imaging was typically applied to assess disease status at 12 and 24 wk. Further detailed description of the trial can be found in *Materials and Methods*. (*B*) Serial monitoring of four melanoma patients following initiation of treatment with pembrolizumab (PEM) (*Left*) or ipilimumab (IPI) (*Right*). Red and gray curves represent CTC scores and serum LDH levels, respectively. (*Upper Left*) Case PEM-25. A 73-y-old woman with diffuse metastatic, $BRAF^{V600R}$ -positive melanoma treated with pembrolizumab, and sustaining a prolonged partial response off therapy. The graph shows response to therapy at clinically indicated 11- and 25-wk evaluations (downward arrows). (*Lower Left*) Case PEM-29. A 63-y-old woman with metastatic, NRAS-mutant melanoma treated with pembrolizumab, which was discontinued due to worsening neurological paraneoplastic symptoms. She was treated with cobimetinib but had further progressive disease and expired. The graph shows clinical progression on PEM at 8 wk (upward arrow). (*Upper Right*) Case IPI-09. A 51-y-old woman with unresectable stage IIIC melanoma treated with ipilimumab, and achieving complete response. She remains off therapy with no evidence of disease. The graph shows clinical response documented at weeks 12 and 20 (downward arrows). (*Lower Right*) Case IPI-03. A 48-y-old woman with unresectable stage IIIC $BRAF^{V600E}$-positive melanoma, treated with ipilimumab. Progression was noted on day 104, and she received pembrolizumab with further progression, followed by dabrafenib and trametinib. After a brief mixed response to targeted therapy, the patient had further progression and expired. The graph shows radiographic progression at week 15 (upward arrow).

Table 1). Of these patients, 48 (98%) had a positive CTC score for at least one measurement during their treatment course (Fig. 2*B* and Table S1). Based on RECIST1.1 criteria at the first (12 wk) clinical monitoring time point, 21 (43%) patients had a response to immune checkpoint inhibition; 21 (43%) had disease progression; and 6 (12%) patients had stable disease, which was sustained for 3–23 mo. Selected CTC response trends are shown in Fig. 2*B*, with all patient data in Tables S1 and S2.

Given the large variability in the clinical course of melanoma patients treated with checkpoint immunotherapy and the difficulty in applying standard radiographic measurements of response, we tested whether blood-based quantitation of CTC burden may provide an early indication of responsive disease. To enable a robust comparison of baseline and on-treatment CTC measurements, we established a prespecified cutoff for the 19 gene CTC score using the median nonzero CTC score derived from the separate initial test cohort of 42 patient samples (low CTC score ≤ 14,732 transcripts per mL of blood, high CTC score > 14,732 transcripts per mL of blood; *Materials and Methods*). In the prospective cohort of 49 patients, 33 patients (67%) had a pretreatment baseline CTC score at or below the prespecified cut point (CTC-low), while 16 (33%) were classified as CTC-high. A comparison of baseline clinical characteristics did not reveal any significant differences between the high or low baseline CTC score groups (Table S3). Notably, the baseline CTC score was not correlated to any of the three clinical outcomes tested: progression-free survival (PFS) ($P = 0.95$, Fig. 3*A*), time to next systemic therapy (TTNT) ($P = 0.72$, Fig. 3*B*), and overall survival (OS) ($P = 0.20$, Fig. 3*C*), all of which were evaluated over a median 24-mo (range, 11–26 mo) clinical follow-up.

We compared the baseline CTC score in each patient with early on-treatment blood draws to test whether a change (ΔCTC score) may reflect initial therapeutic response. Remarkably, patients who exhibited a reduction in CTC score between pretreatment baseline and 6–7 wk of on-treatment (or the closest available draw points; *Materials and Methods*) had significantly improved PFS, compared with patients who had increased CTC scores [hazard ratio (HR), 0.17; 95% CI, 0.05–0.62; $P = 0.008$; Fig. 3*A*]. By 12 mo, up to 64% of patients with increased CTC scores at this early on-treatment measurement experienced disease progression, compared with only 15% of patients with early reduction in CTC scores (Fig. 3*A*).

Change in CTC score between baseline and 6- to 7-wk on-treatment was also significantly related to TTNT. For all patients in this prospective cohort, median TTNT was 18.2 mo (range, 6.3 mo to undetermined): 7.1 mo for patients with an increase in CTC score, and median not reached by the conclusion of the study in patients with a decline in CTC score. Fourteen of 16 (88%) patients with reduction in CTC score remained on therapy for up to 12 mo, whereas 11 of 26 (42%) patients with increased CTC score had to switch therapy due to disease progression within that time (HR, 0.22; 95% CI, 0.06–0.79; $P = 0.02$; Fig. 3*B*).

Furthermore, there was a significant association between the on-treatment reduction in CTC score and improved OS (HR, 0.12; 95% CI, 0.02–0.91; $P = 0.04$; Fig. 3*C*). Patients whose CTC score increased by 6–7 wk had a median OS of 25.7 mo, whereas the median OS was not reached for those with an early on-treatment reduction in CTC score. Eleven of 28 (39.3%) patients with increased CTC scores succumbed to their disease within the study period (median, 24 mo; range, 11–26 mo), whereas only 1 of 16 (6.3%) patients with a reduced on-treatment CTC score died during follow-up (Fig. 3*C*). The significance of the three clinical associations (PFS, TTNT, OS) was validated using a "leave-one-out" cross-validation algorithm (Table S4).

Taken together, in this prospective longitudinal cohort of melanoma patients treated with single-agent immune checkpoint inhibitors, three important clinical parameters: PFS, duration of time to introduction of next-line "salvage" therapy, and overall patient survival on therapy, are correlated with early on-treatment CTC score dynamics. Interestingly, CTC trends were less well correlated with the standard radiographic assessment performed at 12-wk on-treatment. In approximately two-thirds of cases, 12-wk RECIST criteria of response versus progression were concordant with the CTC score assessed at the same time (Tables S1 and S2). Discordant cases may in part reflect the known difficulty in assessing early radiographic changes following immune checkpoint therapy (28), a clinical challenge that stimulated the study reported here. The heterogeneous nature of immunotherapy responses and the surgical and radiotherapy interventions that contribute to clinical care of these patients are described in Fig. 2*B* and Tables S1 and S2. When analyzed together in this pilot study, a decline in CTC score at 7 wk together with a radiographic response at 15 wk are positively predictive of OS in 11 of 11 (100%) patients, while a rise in CTC score together with radiographic progression are correlated with poor survival in 8 of 15 patients (53%), pointing to the potential added utility of combining molecular and radiographic markers of response.

Table 1. Clinical characteristics of prospectively enrolled melanoma patients

Variable	No. (total 49)
Initial therapy	
Ipilimumab	16
Pembrolizumab	33
Age (mean)	63.0 y
Gender	
Female	12
Male	37
Stage (AJCC 7)	
Unresectable stage IIIC	6
Stage IV M1a	4
Stage IV M1b	5
Stage IV M1c	34
Elevated LDH (pretreatment)	
Yes	24
No	22
Unavailable	3
Site of primary	
Cutaneous	34
Mucosal	4
Uveal	2
Unknown	9
Brain metastasis	
Yes	13
No	36
Metastatic sites	
<3	29
≥3	20
Prior adjuvant therapy	
Yes	2
No	47
Prior systemic therapy	
Yes	7
No	42

Clinical features of 49 patients with metastatic melanoma who were longitudinally monitored using the digital CTC score. For each patient, the clinical features are noted at the time of initiation of CTC collection. Individual clinical histories are summarized in Fig. 2*B* and Table S1 (*SI Materials and Methods*).

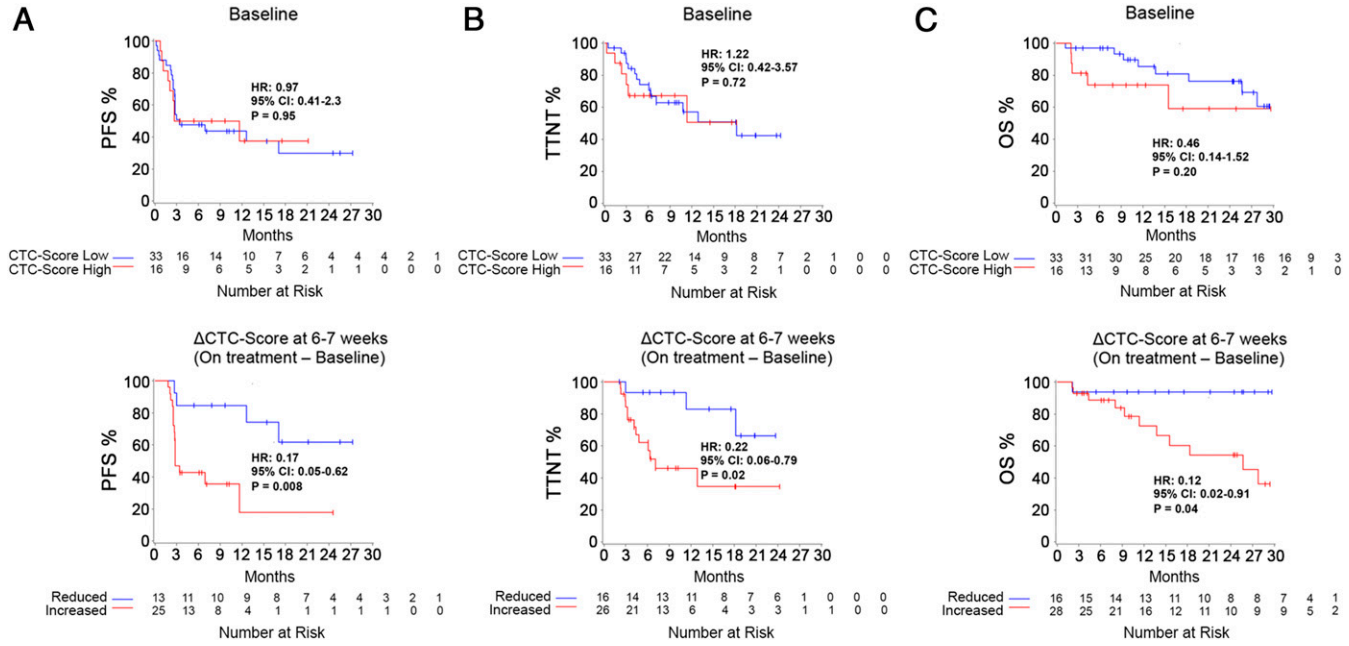

Fig. 3. Associations between early on-treatment change in CTC score and clinical outcome. Kaplan–Meier estimates with numbers of subjects at risk as a function of CTC score at baseline (*Upper*) or changes in CTC score from baseline to 6–7 wk (ΔCTC score, *Lower*). For baseline samples, a threshold CTC score of 14,732 (transcripts number per milliliter of blood) was applied to divide into "CTC score high" (red curves) and "CTC score low" (blue curves). ΔCTC scores were divided into CTC score "increased" (red curves) and CTC score "reduced" (blue curves). Analyses of change in CTC scores were based on a 7-wk conditional landmark approach (36). Hazard ratios (HRs), 95% Wald CIs, and Wald χ^2 *P* values are based on multivariable Cox models. (*A*) Progression-free survival (PFS); (*B*) time to next systemic therapy (TTNT); (*C*) overall survival (OS).

Discussion

In this analysis of prospectively collected blood samples from patients with metastatic melanoma before and during therapy with immune checkpoint inhibitors, we show that longitudinal digital measurements of CTC score are predictive of clinical outcome. Thus, the ability to noninvasively and serially sample tumor cells during the course of immunotherapy may provide an early assessment of response and progression.

Recent advances in microfluidic technologies have enabled the enrichment of CTCs from multiple cancers, independent of their expression of epithelial cell surface markers, a notoriously variable feature of cancer cells (24–26). Replacing microscopic imaging of enriched tumor cell populations with digital RNA-based quantitation of 19 melanoma CTC-derived transcripts now provides a highly sensitive and accurate molecular readout, which is broadly enabling for monitoring tumor cells in the blood circulation (27). Immunotherapy for melanoma is particularly appropriate as clinical proof of principle, since there are currently no established blood-based markers of tumor burden and the neural crest origin of melanoma cells provides multiple unique RNA transcripts that make these cells distinctive within a blood cell background.

Early studies of melanoma CTCs have used RT-PCR analysis of blood samples to amplify melanoma-specific transcripts, some of which were linked to prognosis in patients treated with adjuvant bacillus Calmette–Guérin vaccine (29, 30). However, the general application of this approach has been limited by the inconsistency of RT-PCR amplification from very rare cells within unpurified blood specimens and by the heterogeneity of tumor cells themselves (31). Indeed, even using high-sensitivity digital PCR detection, we found initial enrichment for CTCs to be required for reliable detection, and multiple tumor-derived markers are needed to capture the diversity of expression among tumor cells (Fig. S2*B*).

For patients with metastatic melanoma who are treated with immune checkpoint inhibitors, identifying early and reliable markers of response, as well as predictors of long-term outcome, remains a major challenge with significant clinical implications. For instance, an unfavorable biomarker response could lead to early initiation of combined checkpoint inhibitor therapy, using both nivolumab and ipilimumab, a regimen that leads to improved response rates and PFS, but at the cost of higher toxicity (12, 32, 33). Furthermore, the increasing usage of immune checkpoint blockade in the first-line treatment of *BRAF*-mutant melanoma is associated with the risk that only a subset of patients who would have benefitted from mutation-targeted therapy will in fact have a long-term response to immunotherapy. Thus, rapid identification of *BRAF*-mutant nonresponders to immunotherapy would enable these patients to receive *BRAF*-targeted therapies. Our study is consistent with recent reports of declining circulating tumor DNA (ctDNA) for B-RAF, N-RAS, or KIT mutant alleles in melanoma patients receiving immunotherapy (34, 35). While both ctDNA sequencing and RNA-based detection of CTCs are likely to play important roles in blood-based monitoring of cancer, the use of an expression signature that includes multiple tissue-specific lineage markers shared by virtually all melanomas has the advantage of being independent of mutational status. Only one-half of melanomas have the characteristic *B-RAF*^{V600E} mutation, and blood-based monitoring for other mutations may require initial tumor genotyping followed by individualized mutation profiling. Indeed, CTC RNA signature profiling-based assays may be deployed, irrespective of mutational status, across multiple different types of cancer in which expression of lineage-specific tissue markers enables clear distinction from surrounding normal blood cells.

Taken together, if validated in larger clinical trials, RNA-based scoring of melanoma CTCs may provide a platform for early monitoring of response to diverse immunotherapeutic and molecularly targeted interventions, supporting the rational application of therapy in metastatic melanoma.

Materials and Methods

Patients and Trial Design. All eligible patients had unresectable stage III or IV melanoma and all patients described in this study consented to an Institutional Review Board-approved protocol for CTC collection (Dana-Farber/Harvard Cancer Center protocol 05–300). All patients had *BRAF* mutational analysis performed as part of clinical care, and expanded mutational analysis with a multigene panel was performed in a subset of patients. For the initial test set of the assay, 33 patients donated 18–20 mL of blood at least once during the course of their treatment from 2012 to 2016 (total patient samples, 42; HD controls, 36). For the clinical validation of the assay, a separate cohort of 49 patients was enrolled and monitored prospectively during their treatment with an immune checkpoint inhibitor. Sixteen (33%) patients received ipilimumab (3 mg/kg, i.v., every 3 wk for a planned four doses) as the initial therapy and the other 33 (67%) patients received pembrolizumab (2 mg/kg, i.v., every 3 wk). The blood donation for each patient was planned at the following time points: pretreatment, 3, 6, 9, 12, and 24 wk; and the closest time point was used if the patient was not available at the planned week. The clinical status, immune checkpoint therapy bracketed by the CTC collection, and subsequent treatments are provided in Table 1. Radiographic imaging was performed, per standard of care, at 12-wk intervals or when clinically appropriate (e.g., new symptoms). Response was defined per RECIST1.1 by the treating investigator (R.J.S.).

Microfluidic Enrichment of CTCs. CTCs were isolated from whole blood using the microfluidic CTC-iChip as previously described (24). Biotinylated antibodies against the leukocyte markers CD45 (clone 2D1; R&D Systems) CD66b (clone 80H3; AbD Serotec), and CD16 (Janssen Diagnostics) were added to blood samples collected in EDTA, followed by incubation with Dynabeads MyOne Streptavidin T1 (Invitrogen) to achieve magnetic labeling of leukocytes. Following microfluidic size-based depletion of platelets and red blood cells, leukocytes were magnetically depleted in-flow, and the enriched CTC cell population was collected and frozen in the presence of RNA*later* (Ambion) to preserve RNA integrity.

Statistical Analyses. Detailed statistical analyses are described in *SI Materials and Methods*.

ACKNOWLEDGMENTS. We thank the patients who participated in this study and the Massachusetts General Hospital nurses and clinical coordinators. This work was supported by grants from National Institutes of Health (2R01CA129933, EB008047, and 2U01EB012493), Howard Hughes Medical Institute, National Foundation for Cancer Research, National Science Foundation (DMR-1310266 and ECS-0335715), Harvard Material and Research Science and Engineering Center (DMR-1420570), and Department of Defense and Prostate Cancer Foundation (W81XWH-12-1-0153 and 16YOUN13).

1. Chapman PB, et al.; BRIM-3 Study Group (2011) Improved survival with vemurafenib in melanoma with BRAF V600E mutation. *N Engl J Med* 364:2507–2516.
2. Flaherty KT, et al.; METRIC Study Group (2012) Improved survival with MEK inhibition in BRAF-mutated melanoma. *N Engl J Med* 367:107–114.
3. Hauschild A, et al. (2012) Dabrafenib in BRAF-mutated metastatic melanoma: A multicentre, open-label, phase 3 randomised controlled trial. *Lancet* 380:358–365.
4. Hodi FS, et al. (2010) Improved survival with ipilimumab in patients with metastatic melanoma. *N Engl J Med* 363:711–723.
5. Robert C, et al. (2011) Ipilimumab plus dacarbazine for previously untreated metastatic melanoma. *N Engl J Med* 364:2517–2526.
6. Robert C, et al. (2014) Anti-programmed-death-receptor-1 treatment with pembrolizumab in ipilimumab-refractory advanced melanoma: A randomised dose-comparison cohort of a phase 1 trial. *Lancet* 384:1109–1117.
7. Robert C, et al. (2015) Nivolumab in previously untreated melanoma without BRAF mutation. *N Engl J Med* 372:320–330.
8. Robert C, et al.; KEYNOTE-006 investigators (2015) Pembrolizumab versus ipilimumab in advanced melanoma. *N Engl J Med* 372:2521–2532.
9. Schadendorf D, et al. (2015) Pooled analysis of long-term survival data from phase II and phase III trials of ipilimumab in unresectable or metastatic melanoma. *J Clin Oncol* 33:1889–1894.
10. Topalian SL, et al. (2014) Survival, durable tumor remission, and long-term safety in patients with advanced melanoma receiving nivolumab. *J Clin Oncol* 32:1020–1030.
11. Hodi FS, et al. (2016) Evaluation of immune-related response criteria and RECIST v1.1 in patients with advanced melanoma treated with pembrolizumab. *J Clin Oncol* 34:1510–1517.
12. Larkin J, et al. (2015) Combined nivolumab and ipilimumab or monotherapy in untreated melanoma. *N Engl J Med* 373:23–34.
13. Mahoney KM, Atkins MB (2014) Prognostic and predictive markers for the new immunotherapies. *Oncology (Williston Park)* 28:39–48.
14. Hugo W, et al. (2016) Genomic and transcriptomic features of response to anti-PD-1 therapy in metastatic melanoma. *Cell* 165:35–44.
15. Daud AI, et al. (2016) Programmed death-ligand 1 expression and response to the anti-programmed death 1 antibody pembrolizumab in melanoma. *J Clin Oncol* 34:4102–4109.
16. Le DT, et al. (2015) PD-1 blockade in tumors with mismatch-repair deficiency. *N Engl J Med* 372:2509–2520.
17. Rizvi NA, et al. (2015) Cancer immunology. Mutational landscape determines sensitivity to PD-1 blockade in non-small cell lung cancer. *Science* 348:124–128.
18. Schumacher TN, Schreiber RD (2015) Neoantigens in cancer immunotherapy. *Science* 348:69–74.
19. Johnson DB, et al. (2016) Targeted next generation sequencing identifies markers of response to PD-1 blockade. *Cancer Immunol Res* 4:959–967.
20. Tumeh PC, et al. (2014) PD-1 blockade induces responses by inhibiting adaptive immune resistance. *Nature* 515:568–571.
21. Yu M, Stott S, Toner M, Maheswaran S, Haber DA (2011) Circulating tumor cells: Approaches to isolation and characterization. *J Cell Biol* 192:373–382.
22. Joosse SA, Gorges TM, Pantel K (2015) Biology, detection, and clinical implications of circulating tumor cells. *EMBO Mol Med* 7:1–11.
23. Luo X, et al. (2014) Isolation and molecular characterization of circulating melanoma cells. *Cell Rep* 7:645–653.
24. Ozkumur E, et al. (2013) Inertial focusing for tumor antigen-dependent and -independent sorting of rare circulating tumor cells. *Sci Transl Med* 5:179ra47.
25. Ting DT, et al. (2014) Single-cell RNA sequencing identifies extracellular matrix gene expression by pancreatic circulating tumor cells. *Cell Rep* 8:1905–1918.
26. Miyamoto DT, et al. (2015) RNA-seq of single prostate CTCs implicates noncanonical Wnt signaling in antiandrogen resistance. *Science* 349:1351–1356.
27. Kalinich M, et al. (2017) An RNA-based signature enables high specificity detection of circulating tumor cells in hepatocellular carcinoma. *Proc Natl Acad Sci USA* 114:1123–1128.
28. Wolchok JD, et al. (2009) Guidelines for the evaluation of immune therapy activity in solid tumors: Immune-related response criteria. *Clin Cancer Res* 15:7412–7420.
29. Huang SK, Hoon DS (2016) Liquid biopsy utility for the surveillance of cutaneous malignant melanoma patients. *Mol Oncol* 10:450–463.
30. Koyanagi K, et al. (2005) Multimarker quantitative real-time PCR detection of circulating melanoma cells in peripheral blood: Relation to disease stage in melanoma patients. *Clin Chem* 51:981–988.
31. Krismann M, et al. (1995) Low specificity of cytokeratin 19 reverse transcriptase-polymerase chain reaction analyses for detection of hematogenous lung cancer dissemination. *J Clin Oncol* 13:2769–2775.
32. Postow MA, et al. (2015) Nivolumab and ipilimumab versus ipilimumab in untreated melanoma. *N Engl J Med* 372:2006–2017.
33. Johnson DB, et al. (2016) Fulminant myocarditis with combination immune checkpoint blockade. *N Engl J Med* 375:1749–1755.
34. Lee JH, et al. (2017) Circulating tumour DNA predicts response to anti-PD1 antibodies in metastatic melanoma. *Ann Oncol* 28:1130–1136.
35. Ashida A, Sakaizawa K, Uhara H, Okuyama R (2017) Circulating tumour DNA for monitoring treatment response to anti-PD-1 immunotherapy in melanoma patients. *Acta Derm Venereol* 97:1212–1218.
36. Giobbie-Hurder A, Gelber RD, Regan MM (2013) Challenges of guarantee-time bias. *J Clin Oncol* 31:2963–2969.